JACS
JOURNAL OF THE AMERICAN CHEMICAL SOCIETY
pubs.acs.org/JACS
Article

Stress in DNA Gridiron Facilitates the Formation of Two-Dimensional Crystalline Structures

Lei Yu, Jin Cheng, Dongfang Wang, Victor Pan, Shuai Chang,* Jie Song,* and Yonggang Ke*

Cite This: J. Am. Chem. Soc. 2022, 144, 9747−9752

ABSTRACT: Programmable DNA nanotechnology has generated some of the most intricate self-assembled nanostructures and has been employed in a growing number of applications, including functional nanomaterials, nanofabrication, biophysics, photonics, molecular machines, and drug delivery. An important design rule for DNA nanostructures is to minimize the mechanical stress to reduce the potential energy in these nanostructures whenever it is possible. This work revisits the DNA gridiron design consisting of Holliday junctions and compares the self-assembly of the canonical DNA gridiron with a new design of DNA gridiron, which has a higher degree of mechanical stress because of the interweaving of DNA helices. While the interweaving DNA gridiron indeed exhibits lower yield, compared to its canonical counterpart of a similar size, we discover that the mechanical stress within the interweaving gridiron can promote the formation of the two-dimensional crystalline lattice instead of nanotubes. Furthermore, tuning the design of interweaving gridiron leads to the change of overall crystal size and regularity of geometry. Interweaving DNA double helices represents a new design strategy in the self-assembly of DNA nanostructures. Furthermore, the discovery of the new role of mechanical stress in the self-assembly of DNA nanostructures provides useful knowledge to DNA nanotechnology practitioners: a more balanced view regarding mechanical stress can be considered when designing future DNA nanostructures.

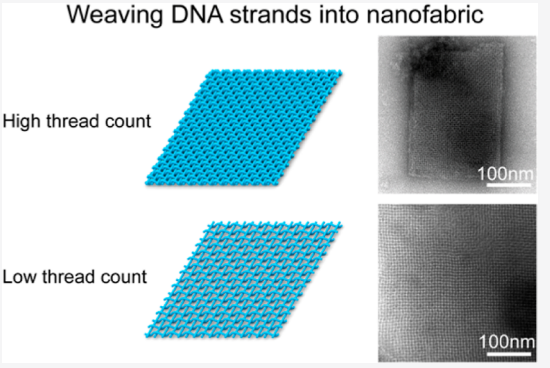

INTRODUCTION

Since Seeman first proposed the feasibility of assembling DNA nanostructures using DNA strands based on the principle of DNA base pairing in the early 1980s,[1] structural DNA nanotechnology has been rapidly developed and enriched by scientists all over the world.[2−4] After decades of development, a rich repository of design methods and nanostructures of controlled sizes and morphologies[5−7] is now available for different applications.[8] From the inception of the field, a cardinal rule in designing DNA nanostructures has been that the mechanical stress within these nanostructures should be minimized,[9,10] except when the stress is intrinsically associated with the design (e.g., the creation of double-crossover tile by rotating and connecting Holliday junctions[9]) or purposefully introduced to generate special morphologies (e.g., to create curvature or twist).[11−14] Time and again, many studies have proved the importance of this fundamental rule, as the yield or the kinetics of self-assembly would decline with the increasing amount of mechanical stress in a DNA nanostructure.[15] Nonetheless, besides being used to induce curvatures and other special geometries in DNA nanostructures, it is reasonable to think that mechanical stress can have other unexplored effects on DNA nanostructure self-assembly. In this work, we carried out a detailed study on the design of DNA gridiron nanoarrays.[16] Specifically, in addition to canonical scaffold-free DNA gridiron, we design a new "half-turn" gridiron with a high-stress weaving conformation: DNA double helices are weaved together to form a nanoarray resembling a piece of interlacing fabric—a structural characteristics distinctively different from the existing DNA nanostructures. The weaving design noticeably reduced the assembly yield of finite-sized gridiron nanoarrays, in good agreement with the principle that mechanical stress lowers the yield of DNA nanostructures, presumably due to the increased potential energy. However, we also discovered that the weaving gridiron design promoted the formation of large two-dimensional (2D) crystalline lattices. In addition, our study on different weaving DNA gridiron nanostructures also revealed that the design could significantly affect the size and geometry of the lattices.

RESULTS AND DISCUSSION

First, we carefully investigated canonical DNA gridiron design (Figure 1). Figure 1a shows the basic design concept for the DNA gridiron structure. The lines represent DNA strands, and

Received: February 21, 2022
Published: May 17, 2022

https://doi.org/10.1021/jacs.2c02009
J. Am. Chem. Soc. 2022, 144, 9747−9752

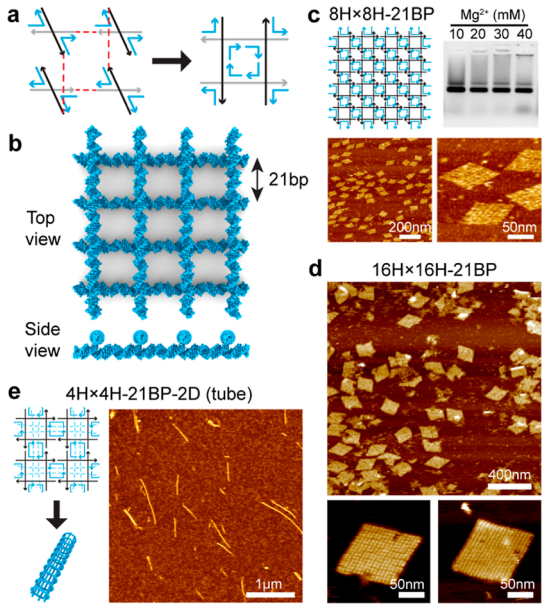

Figure 1. Canonical DNA gridiron nanostructures with full-turn units. (a) Schematic showing the design of a unit of DNA gridiron by connecting four DNA Holliday junctions. (b) Three-dimensional model of a 4H × 4H-21BP DNA gridiron. Each unit is 21 bp by 21 bp. The vertical DNA helices are located on top of horizontal DNA helices. (c) Design diagram, agarose gel electrophoresis, and atomic force microscopy (AFM) images of the 8H × 8H-21BP gridiron. (d) AFM images of the16H × 16H-21BP gridiron. (e) Design diagram and AFM image of the 4H × 4H-21BP-2D (tube) gridiron. It formed narrow nanotubes instead of flat 2D lattices.

the arrows indicate the directional polarity of DNA strands from 5′ to 3′. Different from a previous work of nanoarrays containing Holliday junction units,[17] here, the helices are rotated to connect with adjacent junctions to form a square gridiron unit, and larger gridiron nanoarray can be constructed by including more units. A DNA gridiron can be made with a scaffolded DNA origami method[18] or scaffold-free method, as demonstrated in the original research.[16] A crucial design feature for DNA gridiron is that the length of a DNA helix from one junction to its closest neighboring junction has to be n (n = 1, 2, 3...) full turns of DNA double helices. In this way, all DNA helices would be connected in a relaxed conformation—the constraints caused by the connections at junctions induce minimal mechanical stress. This full-turn gridiron design results in a two-layer conformation, where a set of parallel DNA helices are located on one plane and the other set of parallel DNA helices are located on a different plane (Figure 1b). In this study, we chose to focus only on a scaffold-free DNA gridiron. The primary reason was that DNA origami could not be used to design a weaving DNA gridiron, which contains nicks at the junctions that prevent the inclusion of continuous scaffold DNA strands. For convenience, a DNA gridiron was named [number of horizontal helices(H)] × [number of vertical helices(H)]-[unit size in basepair(BP)]. For example, an 8H × 8H-21BP gridiron is a nanoarray with eight horizontal helices and eight vertical helices, and each square-shaped unit is 21 BP by 21 BP (Figure 1c). We divided the DNA strands into two groups: the black-colored strands that run straight horizontally or vertically are called "x strands", and the blue-colored strands that make turns at the junctions are called "y strands".

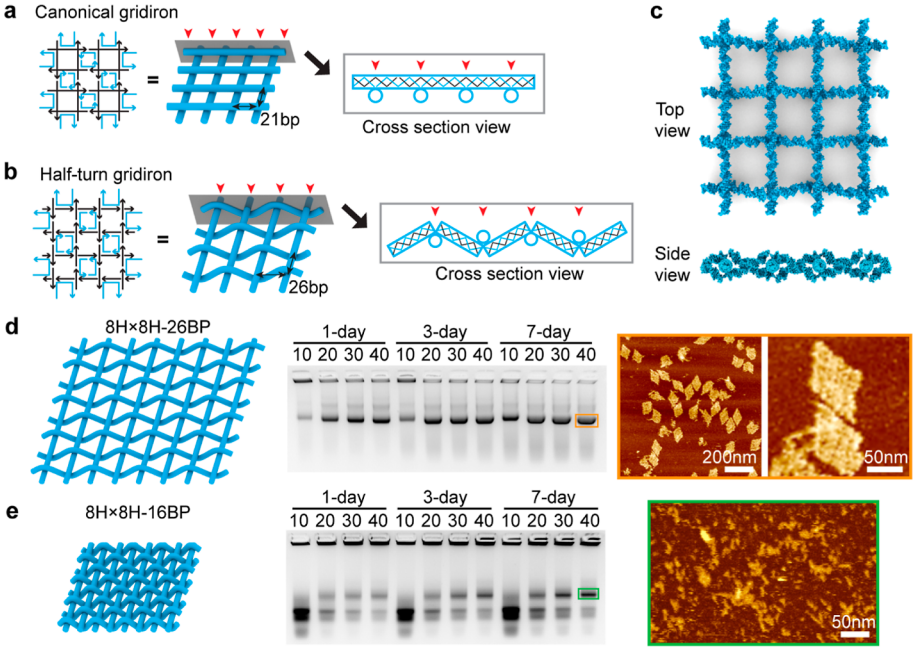

Figure 2. Weaving DNA gridiron nanostructures with half-turn units. (a) Schematic diagrams of the canonical (full-turn) gridiron. The three-dimensional diagram (middle) and cross-sectional view (right) show the two-layer conformation. (b) Schematic diagrams of the half-turn weaving gridiron. The three-dimensional diagram (middle) and cross-sectional view (right) show a weaving conformation. For cross-sectional view, the outlines of DNA helices are displayed as thick blue lines, and the inner zigzag lines represent DNA strands, and red arrows in between indicate the junction points. (c) Three-dimensional models of the weaving gridiron nanostructure. (d) Model, agarose gel electrophoresis under different magnesium concentrations and annealing times, and AFM images of the 8H × 8H-26BP weaving DNA gridiron. (e) Model, agarose gel electrophoresis under different magnesium concentrations and annealing times, and AFM images of the 8H × 8H-16BP weaving DNA gridiron.

https://doi.org/10.1021/jacs.2c02009
J. Am. Chem. Soc. 2022, 144, 9747−9752

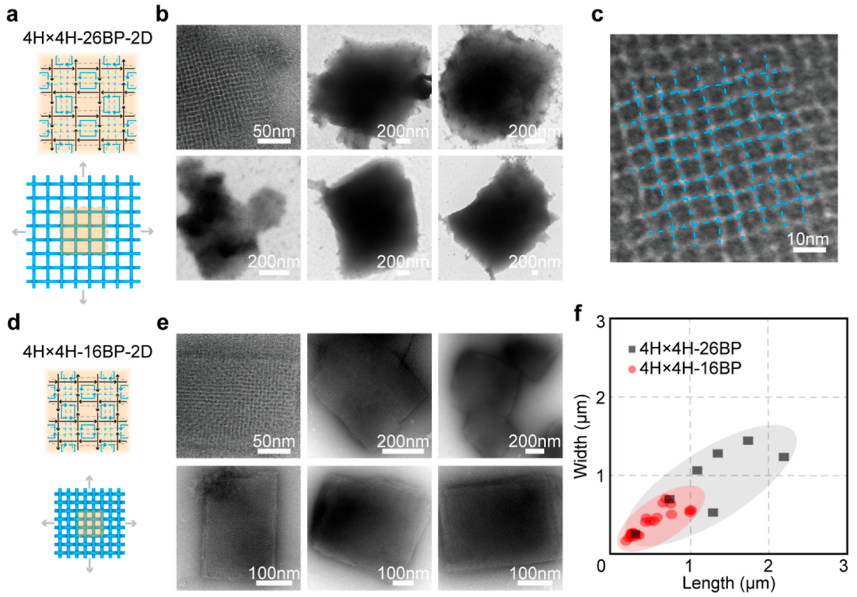

Figure 3. Crystalline lattices assembled from weaving DNA gridiron. (a) Schematic diagrams of the 4H × 4H-26BP-2D weaving gridiron 2D lattice. A repeating unit of 4H × 4H-26BP is shown on top and also marked with light yellow shade in the lattice on the bottom. (b) TEM images of 4H × 4H-26BP-2D weaving gridiron 2D lattices. (c) Zoomed-in TEM image of the 4H × 4H-26BP-2D weaving 2D lattice. Blue dotted lines are added to indicate the traces of DNA double helices. (d) Schematic diagrams of the 4H × 4H-16BP-2D weaving gridiron 2D lattice. A repeating unit of 4H × 4H-16BP is shown on top and also marked with light yellow shade in the lattice on the bottom. (e) TEM images of 4H × 4H-16BP-2D weaving gridiron 2D lattices. (f) Scatter plot of the size of individual 2D lattices. Gray squares represent the 4H × 4H-26BP-2D crystal ($N = 7$) and red dots represent the 4H × 4H-16BP-2D crystal ($N = 24$). For the measurement, we define the longer edge of a rectangle lattice as the length and the perpendicular short edge as the width.

We then tested the assembly yields of canonical gridiron with 21 BP units. The agarose gel electrophoresis of 8H × 8H-21BP gridiron indicated a good yield of the assembly under different concentrations (10−40 mM) of Mg^{2+}. AFM images on the purified 8H × 8H-21BP gridiron further confirmed well-assembled nanostructures (Figures 1c and S1), consistent with previous results.[16] To test the limit of the scaffold-free gridiron, we then designed a large 16H × 16H-21BP nanoarray with a total size of 10,752 basepairs or four times as massive as the 8H × 8H-21BP gridiron (Figures 1d and S2). The yield of this large gridiron decreased significantly in agarose gel electrophoresis assay, even using the optimized isothermal assembly protocol (Figure S2). Nonetheless, a distinct product band (for a sample assembled at 52 °C) was clearly visible and extracted for sample purification and subsequent AFM imaging. Despite the modest assembly yield of 16H × 16H-21BP gridiron, the nanostructure appeared largely well formed and intact in AFM images (Figure 1d). Close inspection of the images revealed that the DNA helices within the gridiron were straight with very minimal distortion. In both the 8H × 8H-21BP gridiron and 16H × 16H-21BP gridiron, the nanoarrays displayed parallelogram shapes instead of square shapes, in agreement with previous results, likely due to the flexibility of the nanoarray.[16]

To test whether large 2D crystalline lattices can be assembled from the DNA gridiron, we designed a periodic gridiron nanostructure by connecting the *y* strands on the edges in a 4H × 4H-21BP gridiron (Figure 1e). The modified design was named 4H × 4H-21BP-2D because the lattice could keep growing horizontally and vertically indefinitely to form large 2D crystalline lattices. However, AFM imaging on assembled samples revealed that this design actually produced relatively narrow nanotubes with a length distribution from a few hundred nanometers to a few micrometers (Figures 1e, S3, and S4). This phenomenon of a 2D DNA lattice forming nanotubes instead was commonly observed in the field of DNA nanotechnology.[19−21] Various mechanisms can lead to the formation of this type of DNA nanotubes. The lattices can contain intrinsic curvature, as demonstrated in an example of DAE-E tile assembly.[19] Another important factor that can promote the formation of nanotubes is the flexibility of a DNA lattice, and it is believed that it is easier for a more flexible lattice to form nanotubes.[20] In the case of 4H × 4H-21BP-2D (tube), the formation of nanotubes was probably the result of both intrinsic curvature and flexibility, although we suspected that the latter might be the primary reason since the tubes are very narrow, with diameters about 20−30 nm, corresponding to two repeating units of the 4H × 4H-21BP gridiron tiles along tube circumference. The nanotubes tended to form large aggregates, especially at relatively high Mg^{2+} concentrations (Figure S4).

After a careful inspection of the DNA gridiron design, we discovered that a different gridiron with a weaving morphology could be created (Figure 2). To achieve this, two important changes have to be made. First, the distance between the two closest neighboring junctions needs to be $n - 0.5$ (n = 1, 2, 3...) full turns of DNA double helices (note that the shortest distance is 0.5 turns of DNA duplex, which works mathematically but is too small in practice). Second, a "nick" needs to be incorporated at each junction to allow the DNA helices to bend to form the weaving pattern. A more detailed comparison between a 4H × 4H-21BP canonical DNA gridiron and a 4H × 4H-26BP weaving DNA gridiron is shown in Figure 2a,b. It is worth noting that the models for weaving gridirons are always displayed in such a way that the vertical helices are straight and horizontal helices are curved because all nicks at the junctions are placed on the horizontal *x* strands. Nonetheless, it is reasonable to believe that the vertical helices are also curved,

https://doi.org/10.1021/jacs.2c02009
J. Am. Chem. Soc. 2022, 144, 9747−9752

likely to a smaller degree compared to the horizontal helices. To better illustrate the design in 3D, we also created these two gridiron nanostructures with 3D design software Tiamat[22] (Figures S5 and S6) and generated 3D models of the 4H × 4H-26BP weaving DNA gridiron (Figure 2c). We then tested the assembly of an 8H × 8H-26BP weaving gridiron by using native agarose gel electrophoresis and AFM imaging (Figure 2d). The analysis based on gel electrophoresis revealed that the yield of the 8H × 8H-26BP weaving gridiron was modest compared to the high yield of the 8H × 8H-21BP DNA gridiron (Figure 1c). We believe an important factor of the relatively low yield of 8H × 8H-26BP weaving gridiron was the higher mechanical stress within the weaving gridiron. This hypothesis was supported by analysis on AFM images of the 8H × 8H-26BP weaving gridiron (Figures 2d and S7). Unlike the 8H × 8H-21BP DNA gridiron, which displays a regular parallelogram geometry, the 8H × 8H-26BP weaving gridiron nanostructures often were more distorted, parallelogram-like shapes. In addition, the individual DNA duplex within the weaving gridiron appeared less straight. Another factor that can reduce the yield of 8H × 8H-26BP weaving gridiron was that its *x* strands were shorter, due to the inclusion of nicks at junctions, than the *x* strands in the 8H × 8H-21BP gridiron. To get a better understanding of how the nicks at junctions and the length of DNA strands affect the assembly yield, we designed an 8H × 8H-21BP canonical gridiron with nicks and studied its assembly (Figure S8). Although this 8H × 8H-21BP gridiron has shorter *x* strands and *y* strands than the 8H × 8H-26BP weaving gridiron, its yield in agarose gel electrophoresis is comparable, if not better, to the yield of 8H × 8H-26BP weaving gridiron. Therefore, the weaving conformation is a significant factor associated with the lower yield of 8H × 8H-26BP weaving gridiron. We then designed and tested an 8H × 8H-16BP weaving gridiron (Figure 2e). Due to its smaller units, we believed that the nanostructure contained a higher level of mechanical stress that would result in an even lower yield. In the agarose gel electrophoresis assay, very small amounts of product bands were observed, even with a 7 day annealing. Furthermore, AFM analysis on the purified 7 day annealed sample extracted from the gel revealed almost no completely assembled gridiron nanostructures (most DNA existed in the gel as aggregates and smaller assembly), although fragments of grid-like nanostructures were observed (Figures 2e and S9). It appeared that the mechanical stress in the 8H × 8H-16BP weaving gridiron was substantial enough to prevent the assembly from producing an observable quantity of complete nanostructures.

Although the finite-sized weaving gridirons showed limited assembly yields, further design and testing of the assembly of 2D crystalline lattices with repeating units of 4H × 4H-26BP or 4H × 4H-16BP weaving gridiron generated large 2D structures (Figure 3). Unlike the finite-sized gridirons (Figures 1 and 2), which were parallelogram-shaped, the horizontal DNA helices were clearly perpendicular to the vertical helices in the crystalline lattices. This observation is consistent with the hypothesis that the parallelogram shape is primarily due to the flexibility of finite-sized gridirons and their interactions with the mica surface during AFM imaging. Once a gridiron grows to a relatively large size, it becomes less likely for the helices in gridiron to move. The 4H × 4H-26BP-2D (Figure 3a) lattices typically grew to a few micrometers in size (Figures 3b and S10). Close inspection on zoomed-in transmission electron microscopy (TEM) images clearly showed that the DNA helices were not straight in the lattices, which might be the result of a combination of factors, including the weaving design, high mechanical stress associated with the design, and distortion induced by the negative staining process (Figure 3c). The overall geometries of the 4H × 4H-26BP-2D lattices were low-aspect-ratio rectangles (close to squares), although the edges of the lattices were typically not very smooth. The assembly of 4H × 4H-16BP-2D (Figure 3d) also produced flat 2D lattices, as confirmed by TEM imaging (Figures 3e and S11). The 4H × 4H-16BP-2D lattices were noticeably smaller than the 4H × 4H-26BP-2D lattices, and most of them were hundreds of nanometers in size (Figure 3f). The smaller sizes of 4H × 4H-16BP-2D lattices were believed to be due to their shorter DNA strands and higher mechanical stress, both of which were also the factors that led to the low yield of finite-sized 8H × 8H-16BP weaving gridiron (Figure 2e). Despite their smaller sizes, the 4H × 4H-16BP-2D lattices exhibited some interesting attributes compared to the 4H × 4H-26BP-2D lattices. The most recognizable differences were the edges of 4H × 4H-16BP-2D lattices were normally much smoother, and therefore, their geometries were more square-like. As discussed earlier, the weaving gridiron design is not symmetric between its horizontal direction and vertical direction due to the placement of all junction nicks on the horizontal *x* strands. Therefore, it is expected that the horizontal helices in a weaving gridiron exhibit a higher degree of curving, which corresponds to a shorter horizontal distance than the vertical distance in a structural repeating unit (the smallest square), although this difference is very small and not measurable in the TEM images. Based on TEM images, it was estimated that the structural repeating unit is on average 6.76 nm by 6.76 nm for the 4H × 4H-26BP-2D lattice and 4.71 nm by 4.71 nm for the 4H × 4H-16BP-2D lattice. All of the measured lengths were smaller than what can be calculated on the basis of the simple models in Figures 2 and 3. This discrepancy was expected since the models did not take into consideration that the DNA helices were substantially bent or twisted in TEM images. The design diagrams and DNA sequences of gridiron used in this work are shown in Figures S12−S19 and Tables S1−S8.

CONCLUSIONS

In summary, we designed and investigated the assembly of scaffold-free DNA gridiron infinite-size nanoarrays and 2D crystalline lattices. Our results showed that the canonical DNA gridiron design could produce large-sized (up to ∼10k basepairs) nanoarray but failed to generate 2D lattices, likely due to the flexibility of the design. In contrast, the new DNA gridiron design with a weaving pattern exhibited noticeably lower yields in the assembly of finite-sized nanoarrays but successfully created flat 2D lattices up to several micrometers in size. Weaving DNA double helices for the self-assembly of DNA nanostructures represents a new design strategy. Besides 2D nanoarrays, the canonical DNA gridiron design was also expanded for building 3D multilayer gridiron.[16] A similar approach can be applied to weaving gridiron to extend these structures into the third dimension. The low yield of, or difficulty in, the self-assembly of weaving gridiron is consistent with the common understanding of the design of DNA nanostructures: the mechanical stress induced by the weaving pattern is expected to increase the potential energy of the products. An important discovery of this work, however, is that mechanical stress can promote the formation of 2D lattices instead of nanotubes. Although the exact mechanism of this

https://doi.org/10.1021/jacs.2c02009
J. Am. Chem. Soc. 2022, 144, 9747−9752

phenomenon is unclear, it is probable that the weaving design and the mechanical stress increase the rigidity of DNA gridirons and thus reduce the tendency to form nanotubes. Other factors, such as the rotational symmetry of the weaving gridiron, can also facilitate the formation of flat 2D lattices through mitigating accumulation of intrinsic curvatures in DNA tiles, as shown in previous works.[20,23,24] We also discovered that the lattice sizes and morphologies (regularity of shapes and smoothness of edges) can be regulated by changing the design of weaving gridiron. The design with a higher degree of mechanical stress produced smaller lattices with more regular shapes and smoother boundaries, likely due to the higher energy states of these lattices. We also believe that this work will shed new light on the role of mechanical stress in the assembly of DNA nanostructures and inspire new development of design strategies that can take a more comprehensive consideration with regard to mechanical stress.

■ ASSOCIATED CONTENT

Supporting Information

The Supporting Information is available free of charge at https://pubs.acs.org/doi/10.1021/jacs.2c02009.

Methods and materials, schematic and characterization images of gridiron structures, and DNA sequences of gridiron structures (PDF)

■ AUTHOR INFORMATION

Corresponding Authors

Shuai Chang − *The State Key Laboratory of Refractories and Metallurgy, the Institute of Advanced Materials and Nanotechnology, Wuhan University of Science and Technology, Wuhan, Hubei 430081, China;* orcid.org/0000-0001-7405-5555; Email: schang23@wust.edu.cn

Jie Song − *Institute of Nano Biomedicine and Engineering, Department of Instrument Science and Engineering, School of Electronic Information and Electrical Engineering, Shanghai Jiao Tong University, Shanghai 200240, China; Institute of Basic Medicine and Cancer (IBMC), Chinese Academy of Sciences; The Cancer Hospital of the University of Chinese Academy of Sciences, Hangzhou, Zhejiang 310022, China;* orcid.org/0000-0002-4711-6014; Email: sjie@sjtu.edu.cn

Yonggang Ke − *Wallace H. Coulter Department of Biomedical Engineering, Georgia Institute of Technology and Emory University, Atlanta, Georgia 30322, United States;* orcid.org/0000-0003-1673-2153; Email: yonggang.ke@emory.edu

Authors

Lei Yu − *The State Key Laboratory of Refractories and Metallurgy, the Institute of Advanced Materials and Nanotechnology, Wuhan University of Science and Technology, Wuhan, Hubei 430081, China; Wallace H. Coulter Department of Biomedical Engineering, Georgia Institute of Technology and Emory University, Atlanta, Georgia 30322, United States;* orcid.org/0000-0002-7107-9137

Jin Cheng − *Institute of Nano Biomedicine and Engineering, Department of Instrument Science and Engineering, School of Electronic Information and Electrical Engineering, Shanghai Jiao Tong University, Shanghai 200240, China*

Dongfang Wang − *Wallace H. Coulter Department of Biomedical Engineering, Georgia Institute of Technology and Emory University, Atlanta, Georgia 30322, United States;* orcid.org/0000-0001-8112-3149

Victor Pan − *Wallace H. Coulter Department of Biomedical Engineering, Georgia Institute of Technology and Emory University, Atlanta, Georgia 30322, United States*

Complete contact information is available at: https://pubs.acs.org/10.1021/jacs.2c02009

Notes

The authors declare no competing financial interest.

■ ACKNOWLEDGMENTS

This work was supported by National Science Foundation grant DMR-1654485 to Y.K. S.C. acknowledges the support from the Outstanding Young and Middle-aged Team in Colleges of Hubei Province of China (T2021002). J.S. is grateful for the financial support from the National Natural Science Foundation of China (no. 22161132008) and the Starry Night Science Fund of Zhejiang University Shanghai Institute for Advanced Study (no. SN-ZJU-SIAS-006).

■ REFERENCES

(1) Seeman, N. C. Nucleic acid junctions and lattices. *J. Theor. Biol.* **1982**, *99*, 237−247.

(2) Seeman, N. C. An overview of structural DNA nanotechnology. *Mol. Biotechnol.* **2007**, *37*, 246−257.

(3) Zhang, F.; Nangreave, J.; Liu, Y.; Yan, H. Structural DNA nanotechnology: state of the art and future perspective. *J. Am. Chem. Soc.* **2014**, *136*, 11198−11211.

(4) Nummelin, S.; Kommeri, J.; Kostiainen, M. A.; Linko, V. Evolution of Structural DNA Nanotechnology. *Adv. Mater.* **2018**, *30*, No. e1703721.

(5) Lin, C.; Liu, Y.; Yan, H. Designer DNA nanoarchitectures. *Biochemistry* **2009**, *48*, 1663−1674.

(6) Ke, Y.; Ong, L. L.; Shih, W. M.; Yin, P. Three-dimensional structures self-assembled from DNA bricks. *Science* **2012**, *338*, 1177−1183.

(7) Zhang, Y.; Pan, V.; Li, X.; Yang, X.; Li, H.; Wang, P.; Ke, Y. Dynamic DNA Structures. *Small* **2019**, *15*, No. e1900228.

(8) Pinheiro, A. V.; Han, D.; Shih, W. M.; Yan, H. Challenges and opportunities for structural DNA nanotechnology. *Nat. Nanotechnol.* **2011**, *6*, 763−772.

(9) Fu, T. J.; Seeman, N. C. DNA double-crossover molecules. *Biochemistry* **1993**, *32*, 3211−3220.

(10) Castro, C. E.; Kilchherr, F.; Kim, D.-N.; Shiao, E. L.; Wauer, T.; Wortmann, P.; Bathe, M.; Dietz, H. A primer to scaffolded DNA origami. *Nat. Methods* **2011**, *8*, 221−229.

(11) Dietz, H.; Douglas, S. M.; Shih, W. M. Folding DNA into twisted and curved nanoscale shapes. *Science* **2009**, *325*, 725−730.

(12) Han, D.; Pal, S.; Nangreave, J.; Deng, Z.; Liu, Y.; Yan, H. DNA origami with complex curvatures in three-dimensional space. *Science* **2011**, *332*, 342−346.

(13) Suzuki, Y.; Kawamata, I.; Mizuno, K.; Murata, S. Large Deformation of a DNA-Origami Nanoarm Induced by the Cumulative Actuation of Tension-Adjustable Modules. *Angew. Chem., Int. Ed.* **2020**, *59*, 6230−6234.

(14) Wang, D.; Yu, L.; Huang, C.-M.; Arya, G.; Chang, S.; Ke, Y. Programmable Transformations of DNA Origami Made of Small Modular Dynamic Units. *J. Am. Chem. Soc.* **2021**, *143*, 2256−2263.

(15) Castro, C. E.; Su, H.-J.; Marras, A. E.; Zhou, L.; Johnson, J. Mechanical design of DNA nanostructures. *Nanoscale* **2015**, *7*, 5913−5921.

(16) Han, D.; Pal, S.; Yang, Y.; Jiang, S.; Nangreave, J.; Liu, Y.; Yan, H. DNA gridiron nanostructures based on four-arm junctions. *Science* **2013**, *339*, 1412−1415.
(17) Mao, C.; Sun, W.; Seeman, N. C. Designed two-dimensional DNA Holliday junction arrays visualized by atomic force microscopy. *J. Am. Chem. Soc.* **1999**, *121*, 5437−5443.
(18) Rothemund, P. W. K. Folding DNA to create nanoscale shapes and patterns. *Nature* **2006**, *440*, 297−302.
(19) Rothemund, P. W. K.; Ekani-Nkodo, A.; Papadakis, N.; Kumar, A.; Fygenson, D. K.; Winfree, E. Design and characterization of programmable DNA nanotubes. *J. Am. Chem. Soc.* **2004**, *126*, 16344−16352.
(20) Ke, Y.; Liu, Y.; Zhang, J.; Yan, H. A study of DNA tube formation mechanisms using 4-, 8-, and 12-helix DNA nanostructures. *J. Am. Chem. Soc.* **2006**, *128*, 4414−4421.
(21) Liu, X.; Zhao, Y.; Liu, P.; Wang, L.; Lin, J.; Fan, C. Biomimetic DNA Nanotubes: Nanoscale Channel Design and Applications. *Angew. Chem., Int. Ed. Engl.* **2019**, *58*, 8996−9011.
(22) Williams, S.; Lund, K.; Lin, C.; Wonka, P.; Lindsay, S.; Yan, H. Tiamat: A Three-Dimensional Editing Tool for Complex DNA Structures. *DNA Computing*; Springer Berlin Heidelberg: Berlin, HeidelbergBerlin, Heidelberg, 2009; pp 90−101.
(23) Winfree, E.; Liu, F.; Wenzler, L. A.; Seeman, N. C. Design and self-assembly of two-dimensional DNA crystals. *Nature* **1998**, *394*, 539−544.
(24) Yan, H.; Park, S. H.; Finkelstein, G.; Reif, J. H.; LaBean, T. H. DNA-templated self-assembly of protein arrays and highly conductive nanowires. *Science* **2003**, *301*, 1882−1884.

https://doi.org/10.1021/jacs.2c02009
J. Am. Chem. Soc. 2022, 144, 9747−9752